



### **Science Arts & Métiers (SAM)**

is an open access repository that collects the work of Arts et Métiers Institute of Technology researchers and makes it freely available over the web where possible.

This is an author-deposited version published in: <https://sam.ensam.eu>  
Handle ID: <http://hdl.handle.net/10985/8327>

#### **To cite this version :**

Baptiste SANDOZ, Alina BADINA, Sébastien LAPORTE, Karene LAMBOT, David MITTON, Wafa SKALLI - Quantitative geometric analysis of rib, costal cartilage and sternum from childhood to teenagehood - Medical and Biological Engineering and Computing - Vol. 51, n°9, p.971-979 - 2013

Any correspondence concerning this service should be sent to the repository

Administrator : [scienceouverte@ensam.eu](mailto:scienceouverte@ensam.eu)



1  
2  
3  
4  
5  
6  
7  
8  
9  
10  
11  
12  
13  
14  
15  
16  
17  
18  
19  
20  
21  
22  
23  
24  
25  
26  
27  
28  
29  
30  
31  
32  
33  
34

**Quantitative geometric analysis of rib, costal  
cartilage and sternum from childhood to  
teenagehood**

Baptiste Sandoz <sup>1</sup>, Alina Badina <sup>2</sup>, Sébastien Laporte <sup>1</sup>, Karene Lambot <sup>3</sup>,  
David Mitton <sup>1</sup>, Wafa Skalli <sup>1</sup>

<sup>1</sup>*Arts et Metiers ParisTech, LBM, 151 bd de l'Hopital 75013 Paris, France*

<sup>2</sup>*Université Paris Descartes, Faculté de Médecine, Hôpital Necker, Service  
d'orthopédie pédiatrique, 149 rue de Sèvre, 75015, Paris, France*

<sup>3</sup>*Université Paris Descartes, Faculté de Médecine, Hôpital Necker, Service de  
radiologie pédiatrique, 149 rue de Sèvre, 75015, Paris, France*

**Corresponding author:**

Dr Baptiste Sandoz  
baptiste.sandoz@ensam.eu

Arts et Metiers ParisTech, LBM, 151 boulevard de l'hopital, 75013 Paris, France

Tel: +33 1 44 24 63 64  
Fax: +33 1 44 24 63 66

**Total word count:** 3699  
**Abstract word count:** 193  
**Number of Figures:** 6  
**Number of Tables:** 1  
**Complementary material:** 1

## 35    **Abstract**

36    Better understanding of the effects of growth on children's bones and cartilage is necessary for  
37    clinical and biomechanical purposes. The aim of this study is to define the 3D geometry of  
38    children's rib cages: including sternum, ribs and costal cartilage. Three-dimensional  
39    reconstructions of 960 ribs, 518 costal cartilages and 113 sternbrae were performed on thoracic  
40    CT-scans of 48 children, aged four months to 15 years. The geometry of the sternum was detailed  
41    and nine parameters were used to describe the ribs and rib cages. A "costal index" was defined as  
42    the ratio between cartilage length and whole rib length to evaluate the cartilage ratio for each rib  
43    level. For all children, the costal index decreased from rib level one to three and increased from  
44    level three to seven. For all levels, the cartilage accounted for 45 to 60% of the rib length, and was  
45    longer for the first years of life. The mean costal index decreased by 21% for subjects over three  
46    years old compared to those under three ( $p<10^{-4}$ ). The volume of the sternbrae was found to be  
47    highly age dependent. Such data could be useful to define the standard geometry of the paediatric  
48    thorax and help to detect clinical abnormalities.

49    ***Keywords:*** *child; rib; cartilage; thorax; sternum*

50

51

## 52 **1. Introduction**

53 The thoracic anatomy of children is clinically important in spinal deformities such  
54 as scoliosis, and anatomical measurements can be used to identify normal  
55 geometry, quantify the severity of deformity, evaluate pulmonary capacity or  
56 build models for orthopedic or surgical treatment. Moreover, the thorax contains  
57 and protects vital organs and can be injured when subjected to impact, as in motor  
58 vehicle accidents. For children, the thorax is the second most often injured  
59 segment in crash events [5].

60 Child external morphology is well known, and some specific databases  
61 have been created to design child dummies [9, 26, 29]. However costal cartilage  
62 and sternal anatomy are generally not assessed, even though they can be of  
63 primary importance. The rib ossification process progressively increases the  
64 stiffness of the thorax and sets final thoracic geometry. During ribcage  
65 ossification, the large difference in material properties between cartilage and bone  
66 affects the stiffness of the rib cage, which is important when considering the  
67 orthotic brace effect or response to an impact in children.

68 Child thorax geometry is often described to highlight specific  
69 abnormalities (scoliosis, pectus carinatum and pectus excavatum), but quantitative  
70 descriptions of child ribcages are rare, while they are essential to build numerical  
71 models or to identify normal patterns for different age groups. Only a few existing  
72 studies provide descriptive parameters of the child rib cage. Derveaux et al. used  
73 2D measurements on lateral X-rays to evaluate the anteroposterior width of the  
74 thorax [11]. On CT-Scan slices, Haller et al. defined an index to describe the ratio  
75 between the transversal and anteroposterior diameters [14], but did not find any

76 correlation with age in a group of 19 patients. Using the same method on 574  
77 child CT-scans, Daunt et al. found a smaller Haller index for children under two,  
78 but a higher index for girls of 0-6 and 12-18 years compared to boys of the same  
79 ages [8]. In 1989, Stokes et al. studied the 3D geometry of 71 scoliotic rib cages,  
80 compared to 10 controls composed of six cadavers and four volunteers (aged 26 to  
81 54), using stereoradiography reconstruction modeling with 0-20° incidences [28].  
82 Costal cartilage dimensions were estimated from direct measurements on four  
83 adult cadavers. Using a similar technique, Delorme et al. studied the effect of  
84 surgical correction on the shape of the ribcages of 29 adolescents (mean age  $15 \pm$   
85 1.5 years) by calculating the 3D rotations of the ribs [10]. Costal cartilages were  
86 not included in the reconstructions. Bertrand et al. performed more precise 3D rib  
87 cage reconstructions on 15 asymptomatic adults (mean age  $27 \pm 8$  years), using  
88 two simultaneous perpendicular planar X-rays from the EOS system (Biospace  
89 Instruments, Paris, France) [3]. While various geometric parameters described the  
90 ribs, the costal cartilage and sternum were not investigated, due to the lack of  
91 visibility. Due to the superimposition of bone structures and the high quantity of  
92 radiotransparent cartilage, it is difficult to have a precise quantitative description  
93 of child cartilage using standard X-rays.

94 Another anatomic part of the thorax is the sternum, which influences the  
95 global stiffness of the rib cage, and can be used as an osseous age estimator. In  
96 1967, Riach found a high age correlation with the surface of the sternebrae in 23  
97 specimens aged between 26 weeks of pregnancy and six-years-old [23].  
98 Nevertheless, the number and time of appearance of the sternebrae show high  
99 variations from one child to another; so it seemed not to be a relevant bone-age  
100 indicator [1, 21-24].

101 To take into account growth of cartilage and bone, it is essential to have a

102 better geometrical description of the child ribcage. Thus, the aim of this study is to  
103 quantify the 3D geometry and to study the age effect of the child rib cage:  
104 including sternum, ribs and costal cartilage, using reconstructions from CT-Scan  
105 data.

106

## 107 **2. Methods**

### 108 **2.1. Population**

109 Forty-eight thoracic CT-scans of children aged from four months to 15 years (22  
110 girls, 26 boys) were collected and anonymized in the Necker Hospital (Paris,  
111 France). The CT-scans had previously been performed on medical prescriptions  
112 with consecutive slices of 4 or 5 mm thickness. The clinical prescriptions for CT-  
113 scans of the thorax were: severe asthma, acute respiratory distress syndrome,  
114 investigation of intrathoracic lymph nodes, inhaled foreign body, trauma with no  
115 bone lesion, staging of primary extrathoracic malignancies. CT-scans in children  
116 with syndromes or heart congenital lesions were excluded. CT-scans showing  
117 thorax abnormalities or recent surgery were not included. Four groups of 12  
118 children were defined according to age: four months to three years (A group), four  
119 to seven years (B group), eight to 11 years (C group) and then 12 to 15 years old  
120 (D group).

### 121 **2.2. 3D reconstruction method**

122 An automatic segmentation and reconstruction of the ribs and ossified sternebrae  
123 was performed on each transversal plane using Avizo software (V5, VSG, USA),  
124 with further manual corrections at the boundaries of the sternebrae. A manual  
125 segmentation of the costal cartilages was accomplished to assess both their shape

126 and the junction to the sternum. This thorough segmentation was performed by a  
127 pediatric orthopedic surgeon previously trained in radiological identifications and  
128 supervised by a pediatric radiologist. A total of 113 sternal sternbrae, 960 ribs  
129 and 518 costal cartilages were reconstructed. The sternal cartilage and some costal  
130 cartilage were not considered because incomplete or too difficult to discern on the  
131 CT-scan images (Table 1). In order to assess the reliability of the resulting  
132 sternbrae volume, 102 sternbrae were reconstructed twice, four weeks apart.

133

### 134 **2.3. Data processing and calculated parameters**

135 From the 3D reconstructions, each rib was modeled by its mid-line, according to  
136 the following steps (Figure 1):

- 137 1. The least square circle of the rib was calculated, defining center O and plane  
138 A.
- 139 2. From the anterior to the posterior extremities, fifty equidistant-angle planes  $P_i$   
140 rotating through O, orthogonal to plane A, were created.
- 141 3. Fifty corresponding cross sections  $S_i$  were calculated as the intersection of  
142 planes  $P_i$  and the external 3D surface of the rib.
- 143 4. The rib mid-line was constructed as the geometric centroid of all  $S_i$  sections.

144 Applied to all left and right ribs, a wireframe of the thorax was then  
145 constructed (Figure 2). A similar method was applied to calculate the costal  
146 cartilage mid-line. Unlike ribs, costal cartilages are not curved in the transversal  
147 plane, so the intersection planes were then defined as parallel to the sagittal plane.

148 Rib cage morphometry was described by three parameters: maximum  
149 anteroposterior width, maximum lateral width, and thoracic index, their ratio. The  
150 local quantitative description of the ribs and the costal cartilage was calculated

151 using rib mid-line length, chord length, enclosed area, maximum width, frontal  
152 and lateral orientations of the rib [3, 7, 16, 18]. In order to estimate the relative  
153 length of the cartilage, the costal index was defined: for each rib, it describes the  
154 ratio between the cartilage mid-line length and the whole costal segment, i.e. rib  
155 and cartilage mid-line lengths.

## 156 **2.4. Statistical analysis**

157 Because no assumption was made regarding the distribution of the data, the  
158 Kruskal-Wallis test was used to assess the statistical significance of differences in  
159 terms of gender, laterality, age group and rib level; with a threshold *p-value* below  
160 0.05 being used to denote significance.

## 161 **3. Results**

### 162 **3.1. Reconstruction assessment**

163 The reproducibility study performed on 102 sternal elements showed a mean  
164 volume difference of 2.7 % (max 9.9 %, Standard Deviation 2.3 %), i.e. 0.2 cm<sup>3</sup>  
165 (max 2.0 cm<sup>3</sup>, SD 0.4 cm<sup>3</sup>).

### 166 **3.2. Sternebrae distribution**

167 Most of the sternums presented a manubrium composed of one sternebra and a  
168 mesosternum composed of three sternebrae. A high variability of anatomical  
169 configurations was found. For example, Figure 3 shows one immature sternum (a.  
170 subject 10; 3-years-old), two sternums with merged sternebrae (b. subjects 33 and  
171 18; 10 and 5-years-old respectively), and two early-adult sternums (c. subjects 26  
172 and 28; 8 and 9-years-old respectively). In three cases, the manubrium had two  
173 ossification centers in a vertical disposition. The uppermost part of the  
174 mesosternum was always composed of a single ossification center. The lowest



175 part of the mesosternum often exhibited lateral or/and longitudinal bifid  
176 ossification centers. The xiphoid process was already ossified in seven cases  
177 before six years old (out of 18 cases).

178 While the distribution of the sternebrae was found to be highly variable, Figure 4  
179 shows the evolution of the sternebrae volumes of each sternum during growth. A  
180 global increase was observed and an exponential equation was fitted to describe  
181 sternum volume versus age relation of the studied population. The volumes were  
182 significantly different between all age groups ( $p < 10^{-4}$ ) and the volume of the 15-  
183 year-old sternum is about 10 times the volume at birth. Furthermore, dispersion is  
184 higher for the oldest patients. No significant difference was found between girls  
185 and boys with regard to the sternal volume distribution ( $p > 0.8$ ).

### 186 **3.2. Ribs and rib cage geometry**

187 Statistical tests did not show significant differences for any parameter, either for  
188 gender ( $p > 0.15$ ) or laterality ( $p > 0.95$ ). Consequently, in the first approach, no  
189 distinction is made between girls and boys, left and right ribs or costal cartilages.

190 The global parameters of the rib cages are summed up in Table 1. The  
191 lateral (LAT) and anteroposterior (AP) widths increase with age, but the thoracic  
192 index shows a very small increase during growth.

193 In Figure 5, the mean and SD costal index is plotted for each rib level by  
194 age group. For all groups, the costal index decreases from rib level 1 to 3 and  
195 increases from level 3 to 7. Furthermore, the costal index is higher for the first  
196 years of life, with an almost equal length of cartilage and bone for levels 1 and 6  
197 (ratio of 47 % and 45 % respectively) for group A. Level 7 has the longest  
198 cartilage region in the youngest group with a ratio of 60 %. For all levels, the  
199 mean costal index decreases significantly by 21 % between groups A (0 to 3 years

200 old) and B (4 to 7 years old) ( $p < 10^{-4}$ ).

201 In Figure 6, the progression of ribcage parameters is plotted by age group  
202 and rib level. Rib area, rib mid-length, maximum width and chord length increase  
203 with age. Rib angles show a small variation in the present population. All the  
204 parameters have a similar pattern of evolution regarding rib level. The statistical  
205 significance of differences between adjacent groups (A-B, B-C and C-D) have  
206 been calculated (Table 2): the geometric rib parameters are significantly different  
207 ( $p < 10^{-4}$ ) between two adjacent groups, except for the frontal and lateral angles.

208 With respect to costal and cartilage parameters, Table 3 (supplementary  
209 material) sums up the mean values and standard deviations of all calculated  
210 parameters. Except for the frontal and lateral orientations of the rib, the mean  
211 values of all costal parameters increase from level 1 to level 6, and then decrease  
212 from level 7 to level 10. Cartilage length increases with the rib level, from level 1  
213 to 7.

214

## 215 **4. Discussion**

216 This study characterizes the bony and cartilaginous structures of the child thorax  
217 during its growth, from CT-scan data. Even if the subjects in this cohort were not  
218 fully healthy, the CT-scans were prescribed for a list of indications that do not  
219 affect the ribcage geometry. Performing CT-scans in healthy children without  
220 clinical indication is not possible due to ethical considerations. In this study, only  
221 CT-scans performed for limited pathologies were collected, while patients with  
222 chest malformations or chronic diseases with potential consequences for the  
223 child's growth were excluded. The dataset is therefore believed to be pertinent to  
224 represent non-pathological geometries of the child ribcage. The number of

225 subjects is large (48) and covers a wide range of ages, from four months to 15  
226 years, with three subjects per year. The gender distribution of the study population  
227 is well balanced. The reconstructions made using the Avizo software have been  
228 validated by an intra-observer reproducibility study on 102 sternbrae. Although  
229 the detection of bone pixels was automatic, an operator correction was required  
230 when two different bone structures were in contact. It was then necessary to  
231 distinguish boundaries manually.

232         As expected, the results show an increase of all parameters with growth.  
233 The originality of this study lies in its quantitative approach. The thoracic index of  
234 the present study shows a slight evolution during growth, up to 11 years; it then  
235 stabilizes (Table 1). Furthermore, the thoracic index shows no significant  
236 evolution between children and adults: Bertrand et al. (2008) evaluated this  
237 parameter at a mean value of 0.63 (SD 0.07) on 15 adults (mean age: 27 years, SD  
238 8 years), whereas the present child population shows a mean thoracic index of  
239 0.65 (SD 0.05). The thicknesses of the ribs were not taken into account in the  
240 present study; therefore the maximum anteroposterior and lateral widths of the  
241 thorax morphometric parameters have been slightly underestimated.

242         The evolution of all the costal parameters for each rib level are compared  
243 to a young asymptomatic adult population [3] (Figure 6). The mean growth speed,  
244 observed as the distance between the different curves of the same parameter, is  
245 not the same between groups, depending on the parameter considered. The  
246 differences between 2 adjacent age groups are significant except for frontal and  
247 lateral angles (Table 2). Because various body parts are known to have different  
248 growth timing [4, 6], no assumptions were made with respect to the growth shape  
249 or the variations between the various parameters, even if global growth was  
250 expected. Therefore due to the similar proportions in the ribcage dimensions

251 between children and adults, child geometric data can be built from that of adults  
252 using an appropriate scaling factor.

253 Comparison of frontal and lateral angles with adults is difficult due to  
254 differences in methodology: while Bertrand et al. studied biplanar X-rays in  
255 standing position, the present study is based on CT-scan data, performed on  
256 children in a lying position [3]. This is the main limitation of this study: CT-scans  
257 were performed in a lying position, together with the unknown respiratory phase  
258 during acquisition. These conditions require a careful interpretation of the angular  
259 parameters of ribs in frontal and sagittal planes, as the effect of the posture on the  
260 thoracic structures (supine versus upright versus seated) has already been  
261 underlined [2, 17]. Similarly, for the youngest children, the presence of clothing  
262 or diaper can change the natural angle of the ribs, as well as the anteroposterior  
263 diameter of the rib cage, as calculated. However, the other parameters are not  
264 affected by the lying position as they are calculated using the rib and cartilage  
265 mid-lines. The costal index presented in this study gives the cartilage length for  
266 the corresponding rib length, for a specific age and rib level. This result - rarely  
267 reported in the literature - is essential in a model design because cartilage is a  
268 chest component with different mechanical properties and behavior from ribs that  
269 are ossified [13]. The current results allow estimates based on *in vivo*  
270 measurements.

271 The sternum is a structure that gradually ossifies. According to the  
272 literature, the number and distribution of sternabrae vary with growth. In 1967, by  
273 taking anteroposterior radiographs of specimens excised at necropsy, Riach found  
274 a correlation between the sum of the sternabrae surfaces and age, especially for  
275 the youngest children, less than six years old [23]. Considering the total volume of  
276 the sternabrae (Figure 4), the present study completes this trend for older children,

277 up to age 15. Contrary to the number of sternabrae, the volume of the bony parts  
278 of the sternum is found to be a good age-predictive parameter, especially for the  
279 youngest. An exponential trend fits with age for the population studied. The  
280 consequences of growth will probably decline after puberty. Due to the high  
281 sensitivity of the results to the age, any conclusion on a gender effect would be  
282 uncertain: the age effect will overwhelm the gender effect.

283         Results from the present study could help to complete missing data or to  
284 validate numerical child models. Indeed, various models from the literature used  
285 X-rays to reconstruct the 3D geometry of the bony structures of the child rib cage  
286 [12, 16]. The costal cartilage, not visible on standard X-rays, is then often  
287 approximated. When geometry is unknown in a child model, it is often scaled  
288 from the adult ones [15, 27, 30]. Besides the known ratio variation of the  
289 geometry and mass of the body segments with growth [6, 25], children's ribcages  
290 contain a substantial quantity of growth cartilage, which has different material  
291 properties. The present results provide new quantitative data on child ribcage  
292 geometry which will assist in building more relevant child numerical models.

293         To refine the interpretation of the results, it would have been interesting to  
294 distinguish between girls and boys according to their respective puberty growth.  
295 However, it then would have been necessary to obtain data on a higher number of  
296 patients that had passed the peak of puberty, until 17 or 18 years old. The same  
297 protocol could be used in further studies for such assessment.

298         Finally, the present study highlighted the cartilaginous preponderance and  
299 the evolution of the young thorax geometry compared to that of adults. Thus such  
300 data could help to improve the biofidelity of child models for the thoracic  
301 segment. Future applications could be considered, like the improvement of Finite  
302 Element Models [19], physical dummies for CPR training [20], forensic analysis,

303 or to define the standard geometry of the paediatric thorax and help to detect  
304 clinical abnormalities.

305

## 306 **Acknowledgements**

307 The authors gratefully acknowledge the kind review of C. Adam. This research was partly funded  
308 by a grant from the ANR (SECUR\_ENFANT 06\_0385) and supported by the GDR 2610  
309 “Biomécanique des chocs” (CNRS/INRETS/GIE PSA Renault).

310

## 311      **References**

312

313

- 314      1.      Ashley G. T. (1956) The relationship between the pattern of ossification  
315                      and the definitive shape of the mesosternum in man. *J Anat* 90:87.
- 316      2.      Beillas P., Lafon Y., Smith F. W. (2009) The effects of posture and  
317                      subject-to-subject variations on the position, shape and volume of  
318                      abdominal and thoracic organs. *Stapp Car Crash J* 53:127-54.
- 319      3.      Bertrand S., Laporte S., Parent S. et al (2008) Three-dimensional  
320                      reconstruction of the rib cage from biplanar radiography. *IRBM*  
321                      29(4):278.
- 322      4.      Beusenbergh M. C., Happee R., Twisk D. et al. *Status of injury*  
323                      *biomechanics for the development of child dummies*. in *Child Occupant*  
324                      *Protection Symposium*. 1993. San Antonio, Texas, USA.
- 325      5.      Brown J. K., Jing Y., Wang S. et al (2006) Patterns of severe injury in  
326                      pediatric car crash victims: Crash Injury Research Engineering Network  
327                      database. *J Pediatr Surg* 41(2):362-7.
- 328      6.      Burdi A. R., Huelke D. F., Snyder R. G. et al (1969) Infants and children  
329                      in the adult world of automobile safety design: pediatric and anatomical  
330                      considerations for design of child restraints. *J Biomech* 2(3):267-80.
- 331      7.      Dansereau Jean, Stokes Ian A. F. (1988) Measurements of the three-  
332                      dimensional shape of the rib cage. *Journal of Biomechanics* 21(11):893.
- 333      8.      Daunt S. W., Cohen J. H., Miller S. F. (2004) Age-related normal ranges  
334                      for the Haller index in children. *Pediatric Radiology* 34(4):326.
- 335      9.      de Jager Kate, van Ratingen Michiel, Lesire Philippe et al. *Assessing new*  
336                      *child dummies and criteria for child occupant protection in frontal impact*.  
337                      in *19th ESV Conference*. 2005. TNO - LAB - BAST - IDIADA - UTAC.
- 338      10.      Delorme S., Violas P., Dansereau J. et al (2001) Preoperative and early  
339                      postoperative three-dimensional changes of the rib cage after posterior  
340                      instrumentation in adolescent idiopathic scoliosis. *European spine journal* :  
341                      official publication of the European Spine Society, the European Spinal  
342                      Deformity Society, and the European Section of the Cervical Spine  
343                      Research Society 10(2):101-7.
- 344      11.      Derveaux L., Clarysse I., Ivanoff I. et al (1989) Preoperative and  
345                      postoperative abnormalities in chest x-ray indices and in lung function in  
346                      pectus deformities. *Chest* 95(4):850.
- 347      12.      Dworzak J., Lamecker H., von Berg J. et al (2010) 3D reconstruction of  
348                      the human rib cage from 2D projection images using a statistical shape  
349                      model. *International journal of computer assisted radiology and surgery*  
350                      5(2):111-24.
- 351      13.      Forman J. L., Kent R. W. (2011) Modeling costal cartilage using local  
352                      material properties with consideration for gross heterogeneities. *J Biomech*  
353                      44(5):910-6.
- 354      14.      Haller J. A., S. Kramer S., A. Lietman S. (1987) Use of CT scans in  
355                      selection of patients for pectus excavatum surgery: a preliminary report. *J*  
356                      *Pediatr Surg* 22(0022-3468).

- 357 15. Irwin Annette L., Mertz Harold J. *Biomechanical bases for the CRABI and*  
358 *Hybrid III child dummies.* in *41st Stapp Car Crash Conference.* 1997.  
359 Lake Buena Vista, Florida, USA.
- 360 16. Jolivet E., Sandoz B., Laporte S. et al (2010) Fast 3D reconstruction of the  
361 rib cage from biplanar radiographs. *Med Biol Eng Comput* 48(8):821-8.
- 362 17. Lafon Y., Smith F. W., Beillas P. (2010) Combination of a model-  
363 deformation method and a positional MRI to quantify the effects of  
364 posture on the anatomical structures of the trunk. *J Biomech* 43(7):1269-  
365 78.
- 366 18. Mitton D., Zhao K., Bertrand S. et al (2008) 3D reconstruction of the ribs  
367 from lateral and frontal X-rays in comparison to 3D CT-scan  
368 reconstruction. *J Biomech* 41(3):706-10.
- 369 19. Mizuno K., Iwata K., Deguchi T. et al (2005) Development of a three-  
370 year-old child FE model. *Traffic Inj Prev* 6(4):361-71.
- 371 20. Nishisaki Akira, Nysaether Jon, Sutton Robert et al (2009) Effect of  
372 mattress deflection on CPR quality assessment for older children and  
373 adolescents. *Resuscitation* 80(5):540.
- 374 21. O'Neal M. L., Dwornik J. J., Ganey T. M. et al (1998) Postnatal  
375 development of the human sternum. *Journal of Pediatric Orthopaedics*  
376 18(3):398.
- 377 22. Ogden J. A., Conlogue G. J., Bronson M. L. et al (1979) Radiology of  
378 postnatal skeletal development - II. The manubrium and sternum. *Skeletal*  
379 *Radiology* 4(4):189.
- 380 23. Riach I. C. (1967) Ossification in the sternum as a means of assessing  
381 skeletal age. *Journal of Clinical Pathology* 20(4):589.
- 382 24. Rush W. J., Donnelly L. F., Brody A. S. et al (2002) "Missing" sternal  
383 ossification center: Potential mimicker of disease in young children.  
384 *Radiology* 224(1):120.
- 385 25. Sandoz B., Laporte S., Skalli W. et al (2010) Subject-specific body  
386 segment parameters' estimation using biplanar X-rays: a feasibility study.  
387 *Comput Methods Biomech Biomed Engin* 13(6):649-54.
- 388 26. Saul Roger A., Pritz Howard B., McFadden Joseph et al. *Description and*  
389 *performance of the Hybrid III three-year-old, six-year-old and small*  
390 *female test dummies in restraint system and out-of-position air bag*  
391 *environments.* in *16th International Technical Conference on the*  
392 *Enhanced Safety of Vehicles.* 1998. NHTSA (National Highway Traffic  
393 Safety Administration).
- 394 27. Schneider K., Zernicke R. F. (1992) Mass, center of mass, and moment of  
395 inertia estimates for infant limb segments. *J Biomech* 25(2):145-8.
- 396 28. Stokes I. A., Dansereau J., Moreland M. S. (1989) Rib cage asymmetry in  
397 idiopathic scoliosis. *Journal of orthopaedic research : official publication*  
398 *of the Orthopaedic Research Society* 7(4):599-606.
- 399 29. van Ratingen Michiel R., Twisk Dirk, Schrooten Mark et al.  
400 *Biomechanically based design and performance targets for a 3-year-old-*  
401 *child crash dummy for front and side impact.* in *Second Child Occupant*  
402 *Protection Symposium.* 1997. Lake Buena Vista, Florida, USA.
- 403 30. Wang Y., Rangarajan N., Shams T. et al (2005) *Design of a biofidelic*  
404 *instrumented 3.4 kg infant dummy,* NHTSA (National Highway Traffic  
405 Safety Administration).



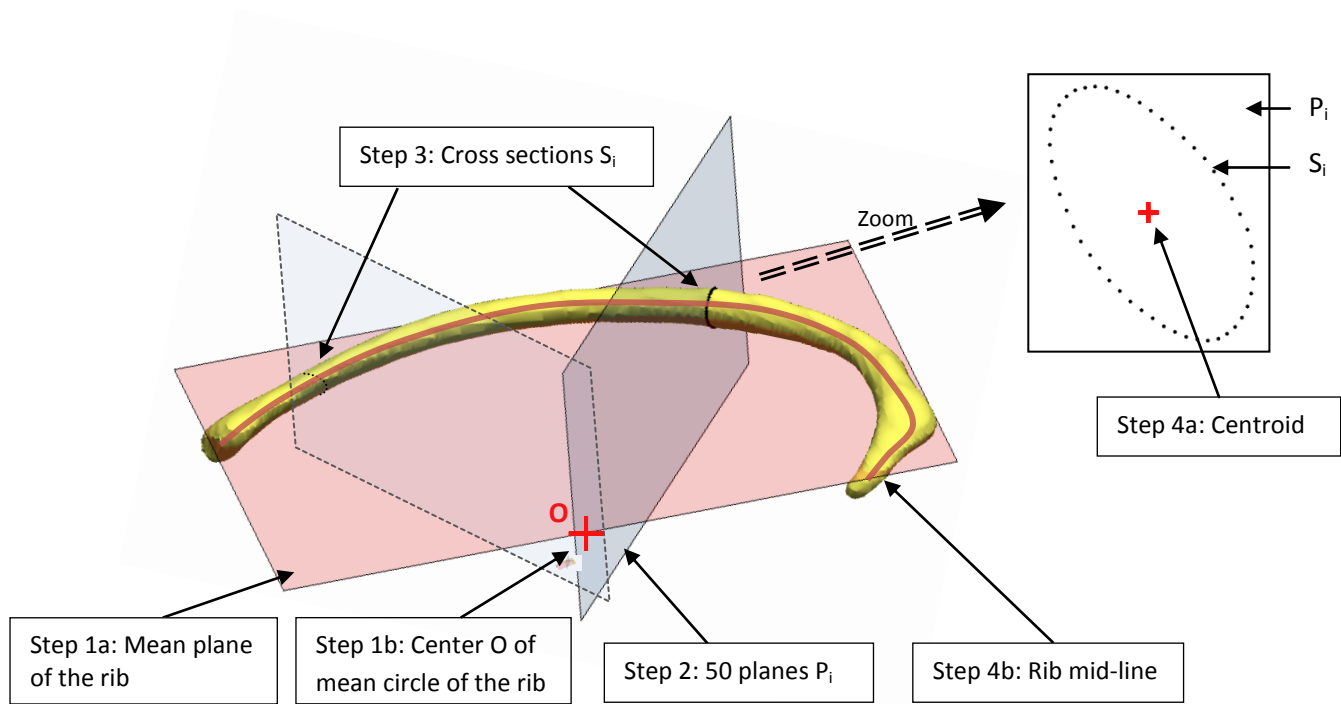


**Figure 1:** Rib mid-line calculation steps.

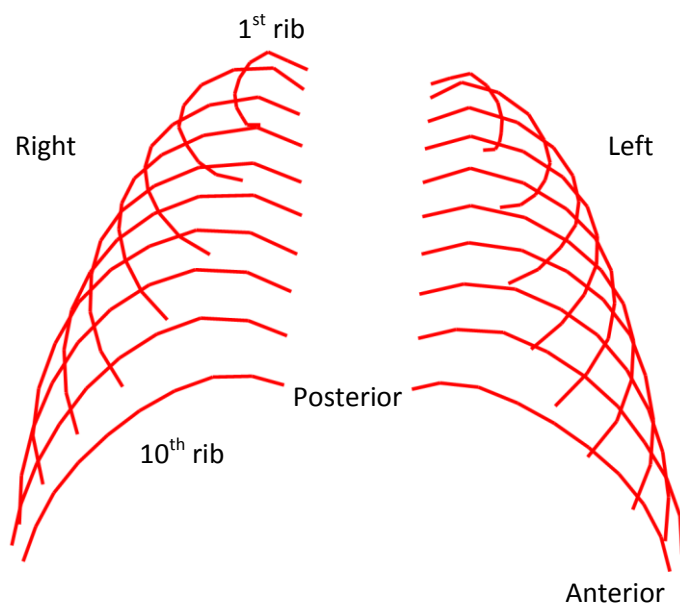


**Figure 2:** Calculated mid-lines rib cage (patient 10).

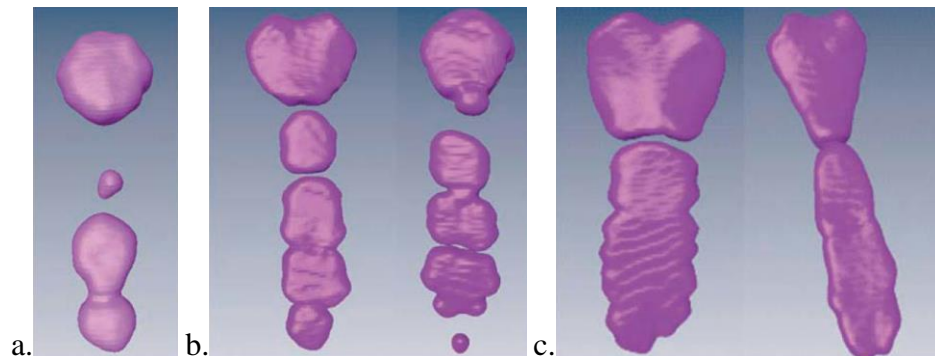


**Figure 3:** Various sternum configurations, high variability not correlated to age.  
a. immature sternum (3 years old); b. merged sternebrae (10 and 5 yo); c. early-adult sternums (8 and 9 yo).

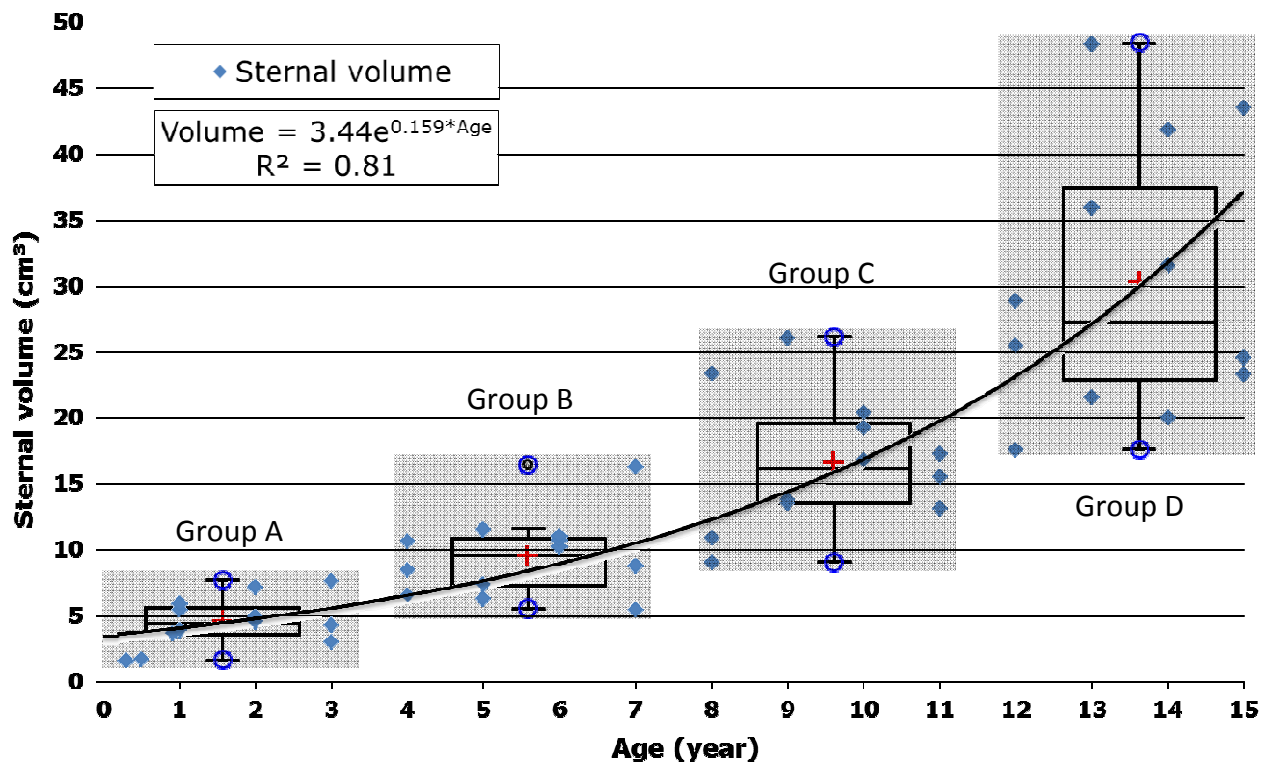


**Figure 4:** Measured sternbrae volume evolution with age, and boxplots by age groups. Group A: 0.3 to 3 years old; Group B: 4-7 yo; Group C: 8-11 yo; Group D: 12-15 yo. The volumes are significantly different between all age groups ( $p < 10^{-4}$ ).

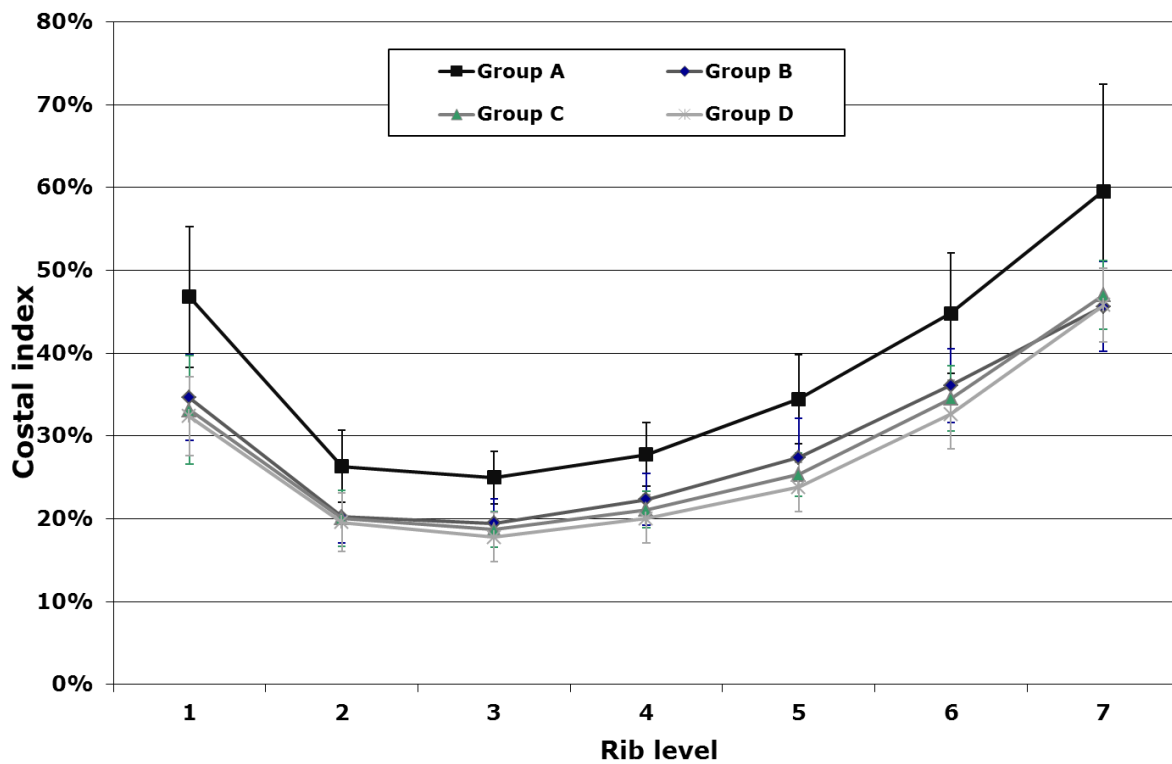


**Figure 5:** Costal index (mean and standard deviation) function of rib level and age group. Group A: 0.3 to 3 years old; Group B: 4-7 yo; Group C: 8-11 yo; Group D: 12-15 yo.

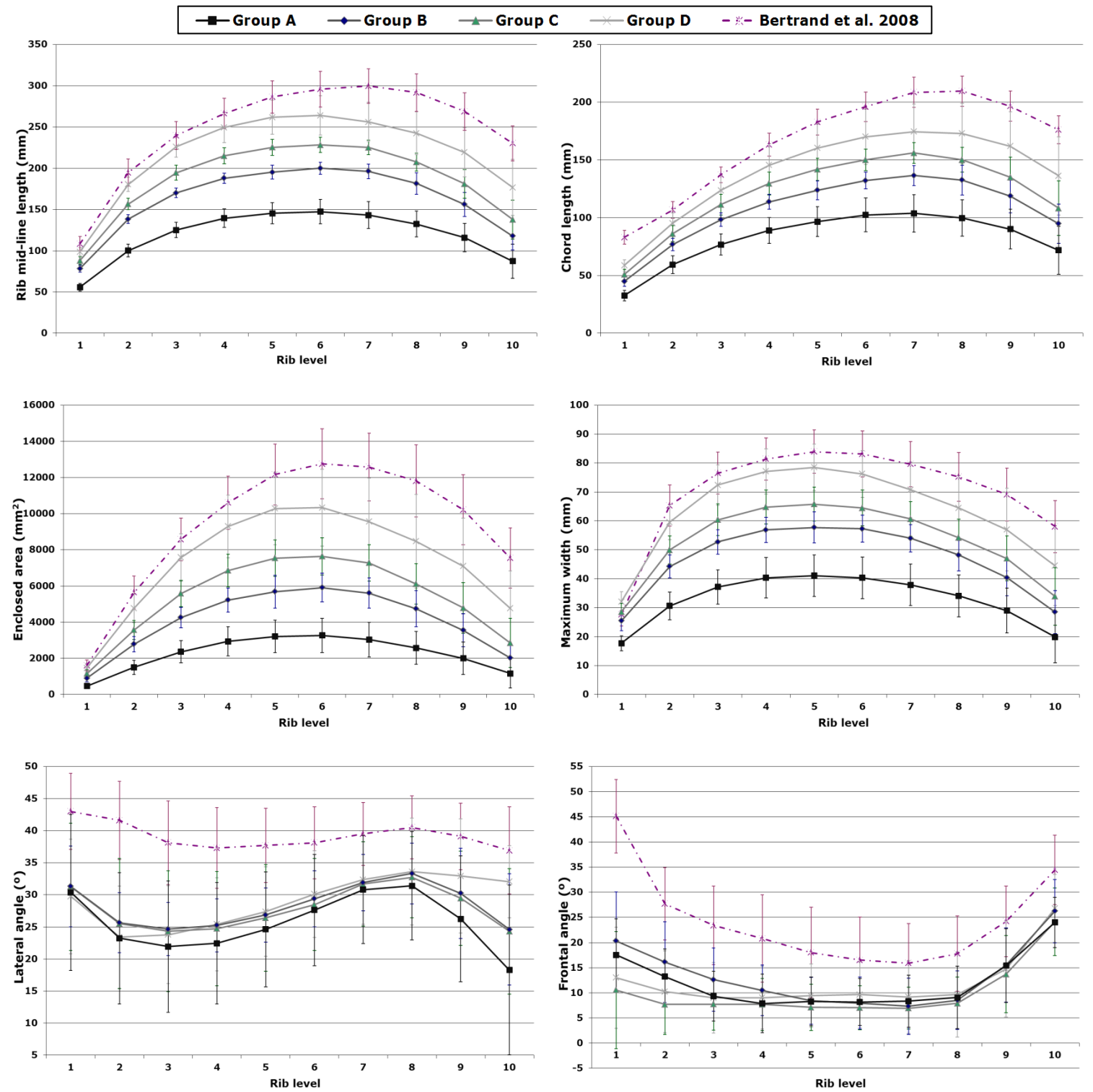


**Figure 6:** Evolution of parameters and comparison with the literature, function of rib level and age group (mean and standard deviation). Group A: 0.3 to 3 years old; Group B: 4-7 yo; Group C: 8-11 yo; Group D: 12-15 yo; Bertrand et al. (2008): 27 yo (SD 8 yo).

Supplementary material - Table 3: Mean (SD) rib and cartilage calculated parameters, 3 children per age group.

		Age (year)															
Data	Rib level	< 1	1	2	3	4	5	6	7	8	9	10	11	12	13	14	15
Rib length (mm)	1	45.0 (5.6)	57.5 (2.9)	58.1 (3.1)	62.9 (1.6)	79.4 (14.1)	76.1 (5.9)	76.1 (3.6)	81.7 (8.5)	86.3 (8.9)	85.5 (7.4)	85.6 (8.8)	94.9 (3.5)	89.6 (9.1)	103.0 (4.7)	100.8 (7.4)	100.8 (7.5)
	2	80.7 (9.4)	100.3 (9.7)	107.3 (5.4)	112.5 (5.3)	131.8 (13.3)	140.4 (8.9)	134.1 (5.1)	146.7 (11.6)	151.4 (12.2)	146.1 (8.9)	159.0 (6.1)	170.1 (3.7)	166.1 (15.0)	189.4 (10.4)	183.9 (9.0)	182.3 (21.1)
	3	99.9 (10.4)	124.9 (10.3)	135.4 (4.7)	140.4 (5.7)	161.6 (13.1)	170.8 (9.6)	166.4 (4.3)	181.6 (10.2)	186.8 (13.9)	184.0 (9.8)	200.2 (3.9)	207.1 (2.1)	206.8 (13.7)	234.2 (18.0)	234.4 (10.7)	228.5 (26.9)
	4	109.1 (11.5)	138.3 (10.9)	152.5 (4.8)	157.3 (6.9)	178.6 (13.2)	188.0 (10.2)	183.4 (4.0)	201.2 (8.7)	205.6 (15.6)	204.1 (11.9)	224.3 (4.5)	225.9 (2.8)	226.5 (16.8)	258.2 (24.1)	262.6 (10.4)	250.5 (29.3)
	5	113.0 (12.1)	144.3 (8.8)	161.4 (4.6)	162.7 (9.0)	186.0 (12.9)	196.6 (10.9)	186.3 (17.4)	212.1 (9.2)	215.3 (17.9)	217.4 (15.4)	235.1 (5.4)	233.5 (4.7)	236.7 (16.4)	275.4 (25.6)	273.8 (10.8)	261.4 (31.2)
	6	112.7 (12.3)	146.2 (6.8)	163.5 (6.0)	166.9 (8.3)	189.2 (13.5)	201.4 (10.5)	195.7 (3.8)	213.9 (10.9)	219.4 (18.3)	220.5 (15.0)	238.5 (3.0)	234.9 (7.5)	239.2 (15.1)	277.4 (31.3)	275.9 (9.5)	263.4 (34.7)
	7	110.2 (12.7)	135.4 (9.4)	160.5 (6.4)	166.7 (7.7)	185.6 (13.3)	194.9 (16.1)	193.1 (3.7)	211.1 (11.2)	215.3 (18.0)	217.9 (15.2)	234.5 (1.8)	233.0 (5.9)	234.1 (13.8)	257.2 (49.5)	270.5 (9.4)	262.3 (35.9)
	8	104.4 (12.4)	122.3 (16.0)	146.9 (10.8)	155.9 (12.3)	177.1 (13.2)	178.2 (25.8)	176.9 (12.9)	193.4 (23.2)	188.2 (12.1)	203.8 (16.1)	225.8 (1.1)	211.9 (16.1)	223.0 (12.0)	233.7 (68.1)	259.0 (9.4)	253.4 (34.5)
	9	95.1 (11.3)	100.9 (20.3)	128.4 (22.3)	139.0 (18.8)	157.6 (7.3)	154.1 (31.8)	155.5 (19.5)	156.9 (25.7)	152.4 (8.4)	180.9 (20.4)	207.6 (5.6)	183.0 (32.6)	202.7 (10.7)	203.7 (85.8)	237.5 (8.2)	233.1 (27.9)
	10	80.9 (8.4)	60.7 (16.9)	97.4 (34.4)	110.6 (25.9)	124.4 (8.8)	115.2 (32.2)	122.8 (20.5)	109.0 (30.8)	103.3 (7.4)	139.0 (20.7)	174.3 (6.7)	140.2 (41.5)	162.6 (9.6)	148.9 (85.8)	199.5 (7.6)	195.6 (19.7)
Cartilage length (mm)	1	22.8 (2.9)	27.2 (0.1)	25.6 (3.6)	27.3 (2.8)	27.0 (0.8)	29.5 (3.0)	24.0 (3.4)	26.6 (1.3)	32.8 (4.2)	29.8 (6.3)	27.2 (5.2)	22.4 (4.1)	28.9 (4.0)	32.7 (3.4)	33.0 (5.5)	32.6 (4.9)
	2	23.7 (3.8)	28.1 (1.0)	27.1 (2.9)	26.8 (2.9)	28.6 (2.5)	26.9 (3.5)	25.9 (5.5)	29.6 (3.6)	32.7 (1.1)	30.8 (6.2)	30.4 (4.1)	28.5 (0.6)	30.9 (4.1)	34.2 (5.0)	37.8 (6.0)	37.4 (5.0)
	3	28.1 (3.6)	34.3 (1.3)	32.1 (2.0)	30.9 (3.2)	35.3 (1.9)	32.2 (5.4)	32.0 (7.2)	33.6 (1.5)	37.6 (2.2)	35.5 (6.2)	35.4 (2.9)	34.4 (1.0)	35.3 (2.6)	39.0 (5.8)	42.4 (6.8)	42.8 (5.9)
	4	34.2 (4.3)	43.3 (1.3)	39.1 (3.4)	38.1 (4.5)	44.5 (1.7)	40.9 (7.0)	42.1 (7.1)	41.7 (2.6)	47.4 (3.2)	44.5 (5.2)	42.8 (3.2)	45.4 (1.4)	45.7 (4.7)	47.8 (5.8)	52.6 (6.7)	52.6 (8.1)
	5	42.5 (4.0)	56.4 (4.4)	48.9 (2.9)	53.7 (10.3)	56.0 (1.9)	52.4 (8.0)	53.9 (8.7)	52.1 (5.0)	59.5 (4.6)	55.4 (4.3)	54.1 (4.6)	57.7 (3.4)	55.6 (2.8)	61.2 (8.3)	65.7 (8.4)	66.0 (9.0)
	6	60.2 (5.5)	73.9 (6.9)	65.6 (2.6)	63.7 (0.7)	76.2 (1.8)	71.5 (11.8)	64.2 (2.1)	74.9 (5.9)	83.2 (3.2)	74.2 (5.5)	75.6 (7.9)	82.7 (4.2)	80.0 (4.4)	78.2 (6.6)	90.7 (9.5)	94.0 (11.0)
	7	70.7 (1.2)		87.1 (2.4)	79.4		98.3 (24.0)	83.6 (4.4)	100.7 (9.3)		105.2 (9.0)	105.7 (10.3)		114.0 (9.0)	110.6 (9.2)	128.7 (7.2)	125.1 (11.1)
Chord length (mm)	1	26.0 (3.1)	34.3 (1.0)	33.8 (2.2)	36.5 (2.2)	44.3 (6.8)	43.9 (2.2)	45.6 (4.7)	45.9 (2.3)	49.8 (5.0)	49.8 (5.0)	48.9 (3.8)	55.1 (1.4)	55.4 (4.4)	62.3 (4.1)	59.9 (4.6)	57.3 (3.9)
	2	47.8 (4.6)	61.3 (2.7)	63.7 (4.8)	64.5 (2.4)	73.1 (5.7)	77.3 (5.1)	77.7 (5.0)	79.1 (4.2)	83.0 (5.0)	82.9 (7.7)	84.5 (3.0)	94.3 (4.9)	92.6 (6.1)	97.9 (5.4)	98.6 (8.7)	92.3 (12.8)
	3	62.9 (3.8)	79.4 (4.8)	82.3 (5.9)	82.6 (2.2)	92.8 (6.6)	99.6 (5.8)	99.6 (4.5)	101.4 (1.8)	108.3 (5.7)	108.5 (12.5)	107.6 (2.5)	120.8 (5.8)	116.6 (5.7)	127.7 (7.6)	131.1 (10.0)	119.2 (19.3)
	4	71.8 (4.3)	92.3 (4.9)	95.3 (6.7)	96.4 (3.6)	107.2 (7.1)	116.0 (6.5)	114.3 (3.4)	117.5 (2.4)	125.8 (7.2)	125.5 (12.9)	127.7 (5.7)	139.2 (6.2)	134.9 (6.9)	152.5 (12.4)	157.1 (14.5)	137.9 (26.5)
	5	77.2 (5.4)	99.4 (5.8)	104.7 (6.9)	105.3 (3.4)	116.6 (7.5)	128.0 (6.6)	121.5 (9.2)	128.9 (2.1)	137.5 (6.8)	136.8 (11.1)	142.4 (7.9)	151.2 (5.7)	147.6 (8.5)	169.5 (13.4)	171.8 (15.3)	152.3 (31.0)
	6	80.7 (6.0)	103.5 (7.1)	111.1 (8.0)	114.4 (2.1)	124.0 (8.0)	135.6 (6.9)	131.8 (1.6)	137.1 (2.6)	146.2 (7.3)	144.8 (11.1)	150.8 (8.0)	158.4 (5.0)	156.0 (8.8)	180.2 (16.8)	182.6 (16.9)	161.3 (36.3)
	7	81.9 (6.7)	99.1 (6.8)	113.8 (7.0)	120.6 (3.6)	128.2 (8.2)	138.8 (11.0)	135.5 (2.1)	143.4 (2.9)	151.5 (7.3)	151.1 (9.6)	157.5 (7.7)	163.9 (5.0)	163.9 (11.3)	176.0 (21.5)	188.8 (15.9)	169.6 (36.5)
	8	80.3 (6.5)	94.4 (10.7)	107.8 (5.6)	116.5 (7.6)	128.5 (10.0)	132.4 (18.6)	129.7 (6.8)	139.7 (13.6)	138.2 (5.3)	148.8 (11.5)	159.2 (4.8)	154.3 (7.1)	163.6 (9.9)	168.2 (37.4)	188.2 (13.3)	171.7 (31.9)
	9	75.3 (6.4)	80.6 (12.9)	97.4 (14.2)	107.2 (12.7)	118.3 (7.4)	119.0 (22.2)	118.3 (11.2)	119.4 (16.8)	116.5 (5.5)	135.0 (15.6)	151.4 (2.2)	136.9 (19.9)	155.0 (7.7)	150.3 (51.1)	179.5 (10.7)	163.1 (26.9)
	10	66.4 (5.0)	53.2 (13.0)	78.3 (23.7)	89.3 (18.4)	98.4 (6.5)	94.1 (23.3)	97.8 (13.2)	88.8 (21.9)	84.7 (5.7)	109.8 (16.5)	132.5 (3.1)	109.8 (28.5)	129.6 (6.6)	115.6 (59.6)	156.8 (9.6)	142.9 (21.7)
Enclosed area (mm <sup>2</sup> )	1	296 (77)	489 (53)	508 (49)	585 (34)	935 (344)	838 (117)	854 (87)	980 (190)	1100 (238)	1077 (180)	1089 (209)	1356 (88)	1213 (248)	1589 (166)	1535 (230)	1504 (203)
	2	969 (231)	1508 (274)	1705 (148)	1838 (188)	2532 (476)	2854 (385)	2630 (231)	3108 (433)	3314 (518)	3099 (331)	3655 (253)	4196 (169)	4068 (714)	5183 (473)	4948 (497)	4878 (1024)
	3	1491 (322)	2332 (355)	2725 (165)	2915 (260)	3834 (562)	4323 (495)	4069 (203)	4811 (483)	5138 (736)	4952 (472)	5899 (304)	6360 (124)	6385 (866)	8118 (1095)	8036 (699)	7789 (1746)
	4	1791 (403)	2843 (419)	3471 (197)	3653 (342)	4728 (649)	5266 (576)	4944 (165)	5945 (464)	6223 (899)	6104 (678)	7459 (399)	7617 (230)	7672 (1146)	10033 (1738)	10061 (706)	9406 (2089)
	5	1929 (433)	3091 (341)	3885 (189)	3928 (449)	5175 (712)	5781 (676)	5152 (862)	6640 (545)	6818 (1114)	6926 (962)	8269 (409)	8130 (365)	8370 (1218)	11385 (1986)	11053 (934)	10335 (2340)
	6	1897 (428)	3150 (222)	3958 (212)	4053 (456)	5325 (772)	6039 (694)	5573 (202)	6716 (687)	6964 (1190)	7033 (1014)	8464 (167)	8095 (558)	8433 (1124)	11467 (2504)	11052 (827)	10395 (2464)
	7	1779 (424)	2681 (393)	3758 (203)	3922 (439)	5087 (761)	5558 (886)	5334 (138)	6455 (766)	6536 (1196)	6726 (1045)	7984 (186)	7852 (327)	7851 (985)	9899 (3857)	10363 (863)	10119 (2307)
	8	1572 (422)	2163 (552)	3138 (480)	3423 (608)	4570 (702)	4583 (1200)	4400 (550)	5412 (1245)	4975 (759)	5800 (922)	7247 (207)	6412 (971)	6973 (740)	8281 (4529)	9279 (889)	9354 (2119)
	9	1292 (362)	1493 (614)	2459 (818)	2761 (779)	3626 (300)	3513 (1339)	3437 (809)	3630 (1126)	3306 (426)	4699 (977)	6203 (437)	4934 (1632)	5778 (640)	6788 (4974)	7797 (716)	8043 (1614)
	10	902 (233)	469 (278)	1482 (962)	1777 (829)	2221 (342)	1958 (1080)	2146 (721)	1751 (912)	1449 (207)	2762 (796)	4394 (371)	3021 (1536)	3669 (445)	4050 (3792)	5590 (426)	5725 (976)
Max width (mm)	1	14.3 (2.2)	18.1 (2.0)	18.3 (0.9)	20.1 (0.8)	26.3 (5.0)	24.1 (1.9)	24.1 (0.8)	27.3 (4.1)	28.5 (3.6)	27.1 (1.9)	28.0 (3.4)	30.6 (2.2)	28.6 (3.8)	33.2 (1.7)	32.3 (2.6)	34.2 (2.7)
	2	24.5 (3.1)	30.3 (3.9)	32.8 (0.8)	35.0 (2.4)	42.6 (4.8)	45.6 (2.9)	41.7 (1.2)	47.2 (4.1)	49.0 (4.7)	44.8 (4.1)	51.6 (1.8)	54.4 (2.5)	53.2 (5.6)	63.6 (4.5)	59.7 (2.5)	61.8 (6.1)
	3	28.9 (3.7)	36.4 (3.1)	40.8 (0.6)	42.7 (2.2)	50.3 (4.8)	53.7 (3.6)	50.0 (0.5)	56.9 (3.1)	57.6 (5.2)	55.6 (5.5)	64.3 (1.9)	64.0 (1.9)	65.5 (5.9)	76.2 (6.7)	72.9 (2.8)	74.9 (7.4)
	4	30.6 (4.1)	38.9 (3.1)	45.3 (0.6)	46.6 (2.4)	54.6 (4.5)	57.2 (3.9)	54.1 (0.9)	61.6 (3.2)	61.2 (5.5)	60.2 (6.2)	70.0 (0.9)	67.7 (2.0)	69.2 (6.7)	80.7 (8.6)	78.7 (2.7)	79.8 (7.0)
	5	31.0 (4.3)	39.9 (2.2)	46.8 (1.2)	46.6 (3.6)	55.6 (4.6)	57.8 (4.2)	54.0 (4.5)	63.4 (3.6)	61.8 (6.4)	62.7 (6.7)	71.0 (0.9)	67.5 (2.5)	70.2 (5.9)	83.1 (9.2)	79.9 (3.9)	80.6 (6.7)
	6	29.9 (4.4)	39.7 (1.4)	45.9 (1.1)	45.8 (3.3)	54.9											